



ELSEVIER

Applied Acoustics 62 (2001) 307–325

**applied
acoustics**

www.elsevier.com/locate/apacoust

Sound transmission through single, double and triple glazing. Experimental evaluation

António J.B. Tadeu *, Diogo M.R. Mateus

University of Coimbra, Department of Civil Engineering, 3030-000 Coimbra Codex, Portugal

Received 17 September 1999; received in revised form 4 April 2000; accepted 18 April 2000

Abstract

Experimental results on sound insulation of glazed openings are reported in this work. The laboratory experiments were performed placing the test specimens between two relatively small rooms. The number of glass panels, their thickness, the air gap thickness between the panels and the type of fixing frame are the variables considered. The insulation conferred by the glazed opening is characterised, identifying the localisation of the dips of insulation in the frequency domain with those related to its own natural dynamic vibration modes and those related to the natural modes of vibration of the rooms. Since the full mathematical description of the acoustic insulation conferred by glazed panels is extremely complicated, simplified theoretical models are frequently used. In this work, the experimental insulation curves obtained are compared with those predicted by the simplified analytical models. This analysis shows that the predictive models, particularly when applied to multiple glazing windows, exhibit marked differences when compared with the experimental data. © 2001 Elsevier Science Ltd. All rights reserved.

Keywords: Vibration; Critical frequency; Resonance frequency; Sound transmission loss

1. Introduction

The transmission of sound energy in a separation element proceeds by the vibration of the element, with the mass and sound frequency being relevant variables. As the mass of the element increases, so does insulation, as a result of increasing forces of inertia. When the frequency of sound incident on an element that maintains the

* Corresponding author. Tel.: + 351-239-797201; fax: + 351-239-797190.

E-mail address: tadeu@dec.uc.pt (A.J.B. Tadeu).

same mass is increased, the vibration power of the element decreases and greater dissipation of sound energy is observed, leading to the rise in acoustic insulation.

Besides these two variables, there are others that may affect the acoustic insulation of a separation element. These include the angle of incidence of the waves, the existence of weak points in the insulation, rigidity, damping of the element and, in the case of multiple elements, the number of panels and their individual characteristics and separation. In a real situation, the transmission of sound between two contiguous rooms depends not only on the separation elements, but also on the connections between the surrounding elements, and on the way in which propagation proceeds inside the emitting and receptor rooms. In this process the vibration eigenmodes of the rooms excited determine the manner of propagation.

The mathematical description of the phenomena involved in acoustic insulation is thus very complex. Studies such as these are usually conducted with variations in only a limited number of the variables in question [1–4]. This results in a set of simplified predictive insulation models. Some of these models are described below since, even though they are simplified, they enable us to understand the acoustic phenomena involved.

2. Acoustic insulation

2.1. Models predicting insulation in single elements

2.1.1. Sound reduction index

If an infinite simple separation element is held to behave like a group of juxtaposed masses, having independent displacement, and null damping forces, the sound reduction index for plane wave incidence follows a law, known as the Law of Theoretic Mass, or the Law of Theoretical Frequency [5],

$$R = 10 \log \left[1 + \left(\frac{\pi f M \cos \theta}{\rho_0 c} \right)^2 \right] \text{dB} \quad (1)$$

where f is frequency (Hz), M is mass per unit area of the panel (kg/m^2), θ is the angle of incidence, ρ_0 is the density of the air ($\approx 1.22 \text{ kg/m}^3$), and c is the velocity of sound in air (for $T = 20^\circ\text{C}$, $c \cong 340 \text{ m/s}$). This equation predicts an increase in the sound reduction index of about 6 dB for each doubling of the mass per unit area.

In practice the panels are not infinite in size and they are struck by an infinite number of plane waves with differing angles of incidence, originating a diffuse field. If a lack of waves at grazing incidence is assumed, the field incidence mass law (or frequency law) can be expressed as

$$R = 20 \log(Mf) - 47 \text{dB} \quad (2)$$

However, the rigidity of the element and its damping affect its dynamic behaviour, leading to localised dips in sound insulation. These can be predicted for frequencies

relative to the normal transversal vibration modes through flexion and due to the propagation of plane waves throughout the panel.

2.1.2. Propagation of bending waves

Bending waves can travel in an infinite plate with a velocity given by [2],

$$c_L = \left(\frac{D\omega^2}{\rho h} \right)^{0.25} \quad (3)$$

where ρ is the density of the material (kg/m^3), h is the thickness of the panel (m), $\omega = 2\pi f$, $D = \frac{h^3 E}{12(1-\nu^2)}$ with E and ν , being the Young's modulus and the Poisson's ratio, respectively. When the wavelength of sound air projected on the plate equals the wavelength of these bending waves, the movement of the panel increases, leading to a low sound insulation. This happens when

$$\omega = \left(\frac{c}{\sin \phi} \right)^2 \sqrt{\frac{\rho h}{D}} \quad (4)$$

where ϕ is the incidence angle of the sound relative to a direction perpendicular to the element.

The critical frequency (f_c) is taken as being that which corresponds to $\phi = 90^\circ$,

$$f_c = \frac{c^2}{1.81h} \sqrt{\frac{\rho(1-\nu^2)}{E}} \quad (5)$$

The resonance dip due to the coincident effect usually begins about an octave below the critical frequency. The amount of the resonance dip depends on the damping of the panel. Below the frequency range of the coincidence, the sound reduction index is determined by the mass law. Above the coincidence zone, the sound reduction index depends on the frequency, which is given by [4, 6]

$$R = 20 \log \left(\frac{\pi f M}{\rho_0 c} \right) + 10 \log \left(\frac{2\eta f}{\pi f_c} \right) \text{dB} \quad (6)$$

where η is the loss factor. This equation indicates, for a constant loss factor, an increase in the sound reduction index of 9 dB/octave above the critical frequency.

The natural vibration modes of the panel are related to its transversal movement in pure flexion, generally at low frequencies, and to the movement of bending waves along the panel, usually occurring at higher frequencies.

2.1.3. Transversal vibration of the panel in pure flexion

As mentioned above, the transversal movement of a panel affects its ability to transfer energy to the surrounding space. The sound striking a separation element

produces a dynamic response, causing insulation dips. These dips in insulation are mainly going to occur at eigenfrequencies related to the pane's flexion-induced transversal movement. If one considers that the thickness of the element is very small, relative to its length and width, the resonant frequencies are given by the following equation, when the element is assumed to be simply supported.

$$f_{nm}(\text{Hz}) = \frac{\pi}{2} \left(\frac{n^2}{a^2} + \frac{m^2}{b^2} \right) \sqrt{\frac{D}{\rho h}} \quad (7)$$

where a and b are the lengths of the wall in direction x and y , respectively, while n and m identify the normal.

The number of resonant frequencies obtainable from Eq. (1) is theoretically infinite. However, only the first vibration modes have a significant influence on the acoustic insulation.

2.2. Models predicting insulation in double elements

The sound insulation of a single separation element may increase if the element is split into two panels separated by an air chamber. However, a double separation element displays additional dips of insulation, due to the dynamic response of the separation element, viewed as two mass layers and an air chamber, and to the resonance frequencies arising from successive reflections (for stationary waves) in the air chamber.

2.2.1. Mass–air–mass resonance frequency

At low frequencies, the double wall can be seen as two masses (m_1 , m_2) acting together as a single panel, in which the air chamber has a negligible effect, and this element behaves like a single element with the same total mass $m = m_1 + m_2$.

As the frequency increases the separation element can be viewed as two mass layers separated by an air chamber that can be close-solved if this model is simplified as a dynamic system constituted by two masses (m_1 , m_2) connected by a spring with rigidity $k = \frac{\rho_0 c^2}{d(\cos \theta)^3}$, where d is the distance between the inner surfaces of the double wall, and θ is the angle of incidence of a plane sound wave. If the rigidity and damping of the panels are disregarded, the problem is further simplified and the resonance frequency can be determined by means of Eq. (8) [7],

$$\omega(\text{rad/s}) = \sqrt{k \frac{m_1 + m_2}{m_1 m_2}} \quad (8)$$

For conditions of normal humidity, a temperature of 20°C, and normal sound incidence, a frequency resonance (in Hz) can be obtained, as in Eq. (9).

$$f_{\text{res}}(\text{Hz}) = 59.8 \left(\sqrt{\frac{1}{d} \left(\frac{1}{m_1} + \frac{1}{m_2} \right)} \right) \quad (9)$$

If the frequency of the sound incident on a double element is higher than the resonance frequency, the air chamber absorbs part of the sound energy, resulting in greater acoustic insulation than is observed in a single element with the same mass. Thus, it could be relevant to have these natural dynamic modes located at relatively low frequencies, (generally below 100 Hz), which, in lightweight panels of normal glass, is only possible for quite thick air chambers.

2.2.2. Multiple reflections in the air chamber

Successive reflections may occur inside the air chamber, generating stationary waves. This phenomenon occurs when the thickness of the air chamber is a multiple of half the wavelength ($n\lambda/2$),

$$f_k = k \frac{c}{2d} (k = 1, 2, \dots) \quad (10)$$

Analysis of Eq. (10), leads to the conclusion that for the first resonance frequency to be outside the zone sensitive to the human ear, the distance between the panels should be small. However, for lightweight panels with small air chambers, the dips in insulation due to its dynamic behaviour as a system of two masses connected by a spring may be significant, as they are generally more important than those caused by multiple reflections within the air chamber.

2.2.3. Sound reduction index

Prediction of sound transmission through double-layer walls has been studied by several authors. London [8] has solved the case of sound transmission through isolated double walls, with identical panels, excited below their critical frequency and mass controlled (that is, the panel resonances need not be considered). Goesele [9] proposed a simplified method to predict the sound transmission loss by double wall, without structure-borne connections and with the gap filled with porous sound absorbing material, when the measured sound transmissions of two constituent single partitions R_1 and R_2 are available.

$$R = R_1 + R_2 + 20 \log \left(\frac{4\pi f \rho c}{s'} \right) \quad (11)$$

where

$$s' = \begin{cases} \frac{\rho c^2}{d} & \text{for } f < \frac{c}{2d} \\ 2\pi f \rho c & \text{for } f > \frac{c}{2d} \end{cases}$$

If no measured sound transmission loss data for the constituent single partitions is available, the sound transmission loss of the double wall can be approximately predicted by

$$R = \begin{cases} 20 \log[(m_1 + m_2)f - 47] & f < 2f_{\text{res}}/3 \\ R_1 + R_2 + 20 \log(fd) - 29 & f_{\text{res}} < f < f_1 \\ R_1 + R_2 + 6 & f > f_1 \end{cases} \quad (12)$$

where R_1 and R_2 are the sound indexes for each layer of the double wall calculated separately (Warnock, 1997).

2.3. Predictive insulation models for triple elements

The acoustic insulation of a triple separation element, like that observed for double elements relative to single ones, is usually higher than the corresponding one for double elements with the same mass. In this case it is not easy to define a simplified mathematical expression to predict the global sound transmission loss. Dips of insulation are again expected to occur at frequencies related to its own natural dynamic vibration modes.

The natural frequencies involved in sound transmission in triple elements are of the same type as those found for double elements, and may be calculated by the formulae already given, with the exception of the natural frequencies related to dynamic behaviour. Taking, in this case, a simplified system of three masses (m_1 , m_2 , m_3) attached to each other by springs with rigidity k_1 and k_2 , Eq. (13) can be defined, and this can be solved to give the natural frequencies of the system [10].

$$[m_1 m_2 m_3](\omega^2)^2 - [k_1 m_3(m_1 + m_2) + k_2 m_1(m_2 + m_3)](\omega^2) + [k_1 k_2(m_1 + m_2 + m_3)] = 0 \quad (13)$$

with $k_1 = \frac{\rho c^2}{d_1}$ and $k_2 = \frac{\rho c^2}{d_2}$, where d_1 and d_2 are the thickness of the air chambers.

2.4. Dynamic response of a parallelepiped room

The precise characterisation of a sound field, which is established in an enclosed space, in the presence of a sound source, is not an easy task. It requires complex physical-mathematical treatment and involves variables, which are difficult to quantify, such as the characteristics of sound energy dissipation in the air and the surrounding medium, and those of the sound sources [11–13].

The vibration properties of an enclosed space, owing to the formation of stationary waves, depend on the shape and geometrical dimensions of the elements of the surroundings as well as of the boundary conditions throughout the surroundings as a whole. Taking a parallelepiped room, with dimensions L_x , L_y and L_z , the equation of equilibrium that governs the waves of sound pressure in the room (Helmholtz equation) leads to Eq. (14), which allows us to obtain the natural frequencies of the room,

$$f_{nmp} = \frac{c}{2} \sqrt{\frac{n^2}{L_x^2} + \frac{m^2}{L_y^2} + \frac{p^2}{L_z^2}} \quad (14)$$

where c is the velocity of sound propagation in the air (m/s), and n , m and p represent the number of the eigenmode, according to x , y and z , respectively.

Notice that the first eigenfrequencies for large spaces are registered for very low frequencies, while for small spaces these frequencies are higher.

3. Experimental

3.1. Preparation of the rooms

The experimental work entailed studying the behaviour of glazed openings subjected to variations in acoustic pressure. Two testing compartments were specially prepared. The dimensions of these compartments were defined so that they were similar to small rooms inside dwellings ($4.0 \times 2.7 \times 2.7 \text{ m}^3$ and $3.0 \times 2.7 \times 2.7 \text{ m}^3$). This work had to be carried out in acoustic conditions to permit control of the variables in play. The first phase consisted of construction work to build two contiguous rooms that would guarantee a high degree of acoustic insulation (if we disregard the opening for testing samples). The separation between the two rooms was made in such a way as to hold the testing samples ($1.48 \times 1.45 \text{ m}^2$), to ensure a high degree of insulation between the two rooms outside the area occupied by these samples, and to create conditions in which flanking transmissions would be negligible. In a second phase, some absorbent elements were placed in the receiving room, to diminish reverberation in that room. The insulation of testing samples was not obtained directly, from the difference between the sound levels in two rooms, (pure acoustic insulation), but rather by taking into consideration the reverberation phenomena in the compartments, following the Portuguese Standard NP-2073 [14].

$$D_c = L_1 - L_2 + 10 \log \left(\frac{10T_r}{0.16V} \right) \quad (15)$$

where L_1 and L_2 are the average sound levels (dB) in the emitting and receiving chambers, respectively, V is the volume of the receiving chamber (m^3) and T_r is the average reverberation time (s) for a given frequency.

Before placing the specimens inside the opening of the separating wall, a rubber screen, 5 mm thick, was glued all round the edge of the opening to permit better bonding of the specimen to the opening. The glass panes applied were as close as possible in size to the opening and the edges were sealed with a silicone strip on both sides of each panel. The characteristics of the glass panes, determined by laboratory tests (modulus of elasticity, $E=72 \text{ GPa}$, Poisson's ratio $\nu=0.22$, mass density $\rho=2500 \text{ kg/m}^3$), are not described in this article for reasons of brevity.

3.2. Experimental conditions

The whole system for capturing sounds and vibrations, as well as the position of the transducers and the source, is shown diagrammatically in Fig. 1. The chain of

measurement was composed of three essential parts: transducers; signal amplifiers/conditioners, and a data acquisition board.

The transducers used were Brüel & Kjaer microphones and accelerometers, types 4155 and 4371, respectively. Signal amplification/conditioning was done using Brüel & Kjaer conditioner, type 2525 and the pre-amplifier type ZC0020 provided by the AC output of the Brüel & Kjaer modular precision sound level meter, type 2231.

The data acquisition board (Keithley Metrabyte, type DAS - 40G2, 12 bits) was installed inside a personal computer. It allows a maximum reading of 16 channels with a total maximum sample, for all channels, of 250 000 samples per second.

Before any test was performed, the chain of measurement was calibrated and the appropriate processes for transforming the acquired data to sound level and acceleration were defined. Calibration of the sound level measuring circuit was done with the help of two Brüel & Kjaer calibrators, type 4230 and 3541, emitting, respectively, 94 dB at 1000 Hz and 124 dB at 250 Hz. A Brüel & Kjaer type 4924/WH2606 calibrator was used to calibrate the vibration measuring circuit, vibrating with an acceleration of 3.16 m/s^2 at 159.2 Hz.

After complete calibration of the chain of measurement, the test samples were positioned, and the capture points of the vibrations of the glass and the sound pressure in each room selected. A standardised sound source (Brüel & Kjaer type 4224) was then placed in the emitting room, emitting a sound characterised by its “Wide Band” frequency spectrum.

Neither the sound nor the vibrations could be measured correctly if the position of the transducers and the excitation source were not chosen with great care [15]. For example, an accelerometer placed on the centre of the glass panel does not detect the vibration mode caused by transversal vibration, occurring through flexion of the panel, for which this point does not move.

The sound pressure was captured simultaneously in both rooms, at ten positions distributed around the interior of each room, with a sampling interval of $50 \mu\text{s}$,

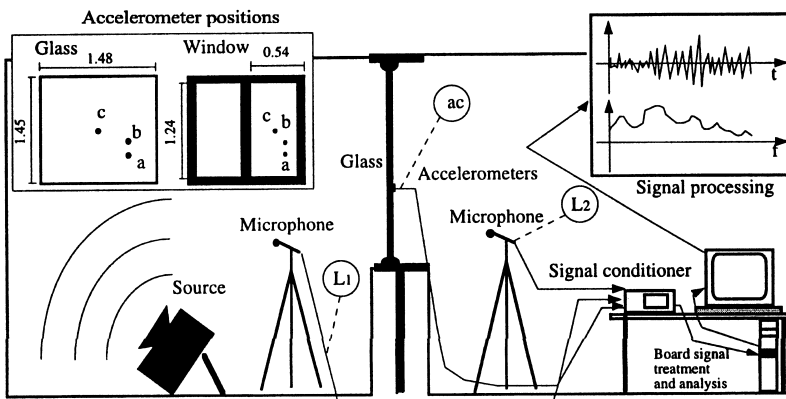


Fig. 1. Scheme of the rooms and the acquisition system used.

allowing a frequency spectrum with a resolution of 0.15 Hz. The average frequency spectra were calculated from the 10 spectra generated.

The results obtained from the system of capture shown in Fig. 1 were first processed using the fast Fourier transform, which allowed the data to pass to the frequency domain. Programs developed for dividing the spectrum into frequency bands and determining a mean curve of acoustic insulation were used later.

3.3. Type of test samples

This work looks at two distinct types of tests: one in which only the glass panels, single or multiple, are tested, and the other in which the same kind of glass is tested, but inside two different window frames.

In the tests on glass without frames, two types of glass were used: one 4 mm thick and the other 8 mm thick, in a variety of combinations and with different air chambers, as shown in Table 1.

The tests on glass inside frames were carried out using two kinds of frames, both with single glass panels 8 mm thick. With this type of test we were only attempting to observe the dips of insulation introduced by the frame itself. The first solution consisted of using a “good quality” frame with very good seals, and with two opening panes and central reinforcement. The second solution, frankly worse in terms of acoustics, comprised a frame with two sliding panes, with light mass, like most of those used in buildings in Portugal today.

Table 1
Glazed solutions tested (without frame)

Type of glazed solution	Sample	Thickness 8 mm	Thickness 4 mm	Thickness 4 mm	Air gap 1 (in mm)	Air gap 2 (in mm)
Single	1	– ^a	+ ^b	–	–	–
	2	+	–	–	–	–
	3	+	+	–	2.5	–
	4	+	+	–	10	–
	5	+	+	–	20	–
	6	+	+	–	35	–
Double	7	+	+	–	50	–
	8	+	+	–	100	–
	9	+	+	–	200	–
	10	–	+	+	10	–
	11	–	+	+	50	–
	12	+	+	+	10	10
Triple	13	+	+	+	100	10
	14	+	+	+	100	50

^a – Not used.

^b + Used.

4. Relevant results

A wide range of laboratory tests was performed. Figs. 2–10 display some of the experimental results obtained, to illustrate the main findings. These plots were built up with the help of the experimental insulation results (in bands of 1/10 octave). The acoustic insulation expected from the models for single and double elements, described in this paper, the acceleration spectra of the transversal movement of the glass panels at the central point of each panel (point C), the position of the natural

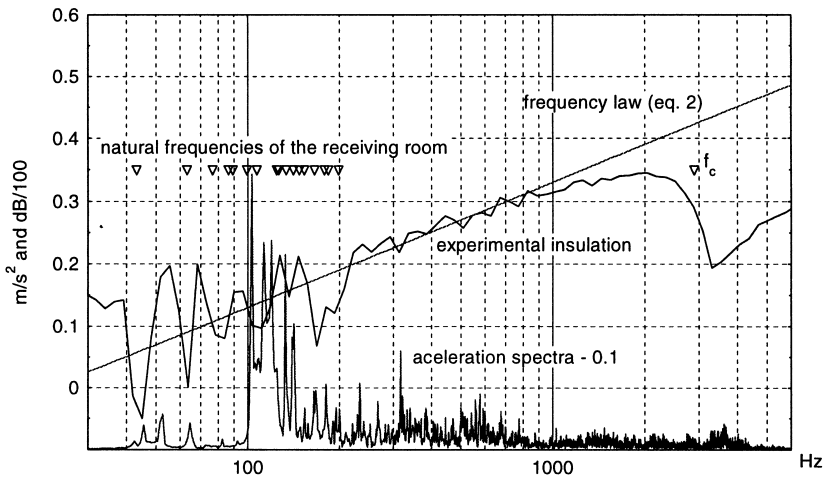


Fig. 2. Insulation and vibration curves. Single 4 mm glazing solution.

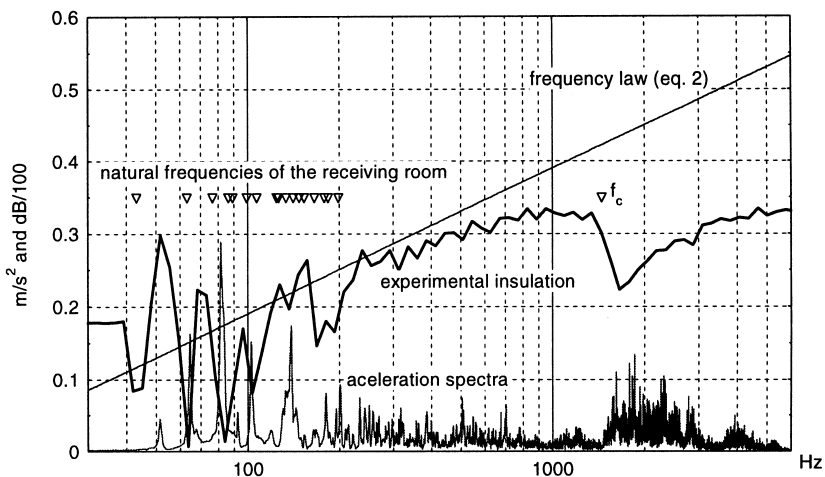


Fig. 3. Insulation and vibration curves. Single 8 mm glazing solution.

frequencies of the rooms, calculated analytically, and the localisation of the dips of insulation resulting from the simplified dynamic behaviour of the panels (f_c , f_{res} , f_k) are displayed when it enables the reader to better understand the results.

Analysis of the results reveals that, for very low frequencies, there is a marked dependency between the insulation curves for the different glazed solutions tested, and the form of propagation inside the receptor room. These results are not particularly surprising since the dimensions of each test room are significantly smaller than what is experimentally defined as desirable (around 30 m³ for the receptor and 24 m³ for the emitting room). Similar behaviour was found by Tang et al. [16], in the work he developed to analyse the sound transmission through close-fitting finite

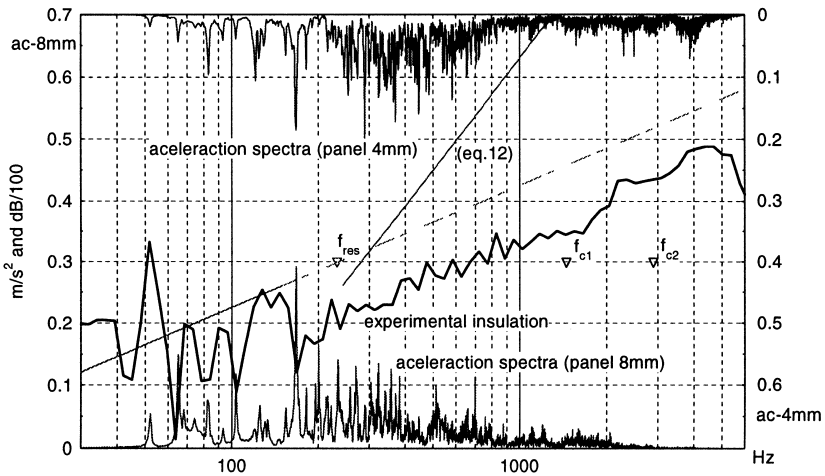


Fig. 4. Insulation and vibration curves. Double [8 + (10) + 4] mm glazing solution.

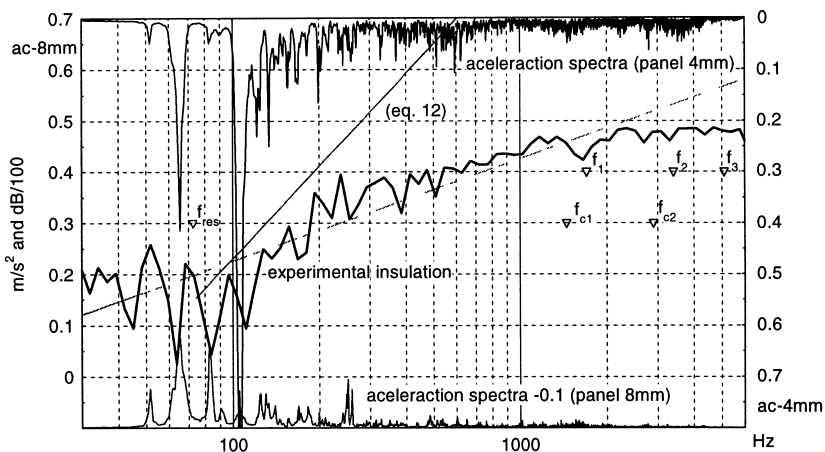


Fig. 5. Insulation and vibration curves. Double [8 + (100) + 4] mm glazing solution.

sandwich panels. In his work, an open rectangular concrete box (368 × 368 × 620 mm) was built, and the test panels were fixed over it. The cavity-controlled modes, defined by the size of the concrete box cavity, made by far the greatest contribution to the sound field.

Figs. 2 and 3 present the results obtained for single glazed solutions, 4 and 8 mm thick, respectively, when the equivalent sound pressure level L_{eq} measured in the emitting room reached 110 dB(A). In both figures, small triangular marks were

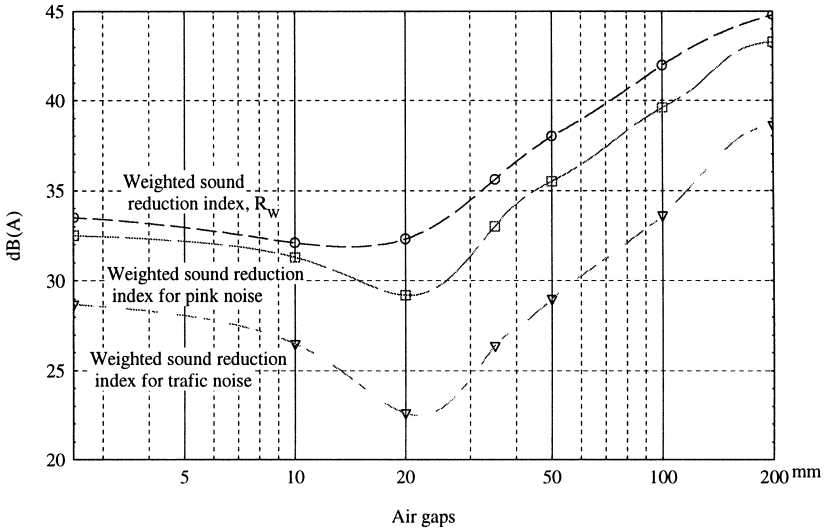


Fig. 6. Weighted sound reduction indexes in double [8 + 4] mm glazed solutions. Different air chamber thicknesses.

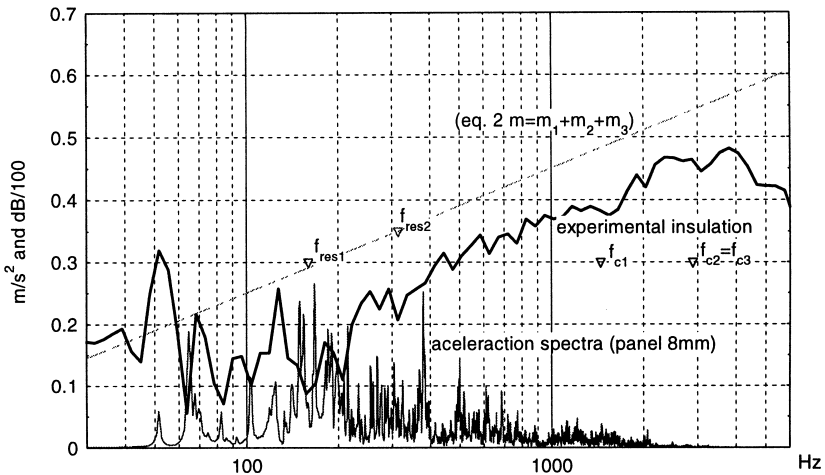


Fig. 7. Insulation and vibration curves. Triple [8 + (10) + 4 + (10) + 4] mm glazing solution.

added to identify the lowest natural frequencies of the room given by Eq. (14). It can be observed, in fact, that the insulation curves show dips at frequencies, not coinciding with the energy dips of the sound source, but with the resonance frequencies of the receiving chamber, conditioning sound insulation at low frequencies. It can be further observed that the vibration of the glass panes at low frequencies also depends on the natural excited frequencies of the receiving and emitting rooms.

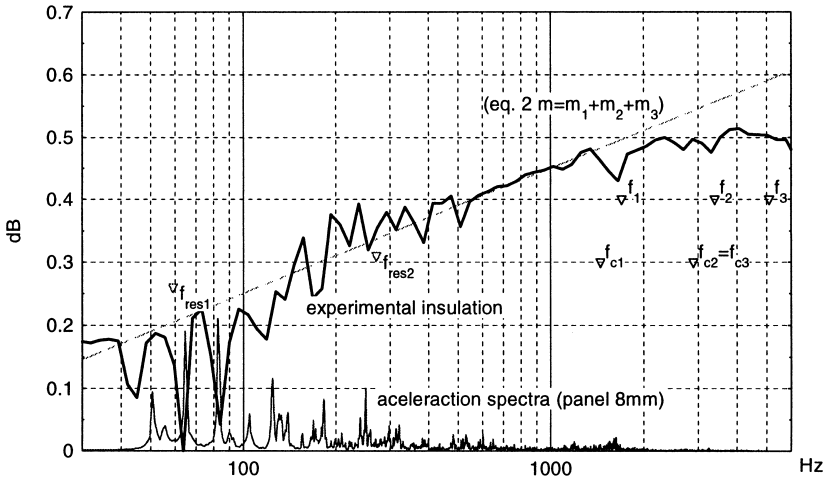


Fig. 8. Insulation and vibration curves. Triple [8 + (100) + 4 + (10) + 4] mm glazing solution.

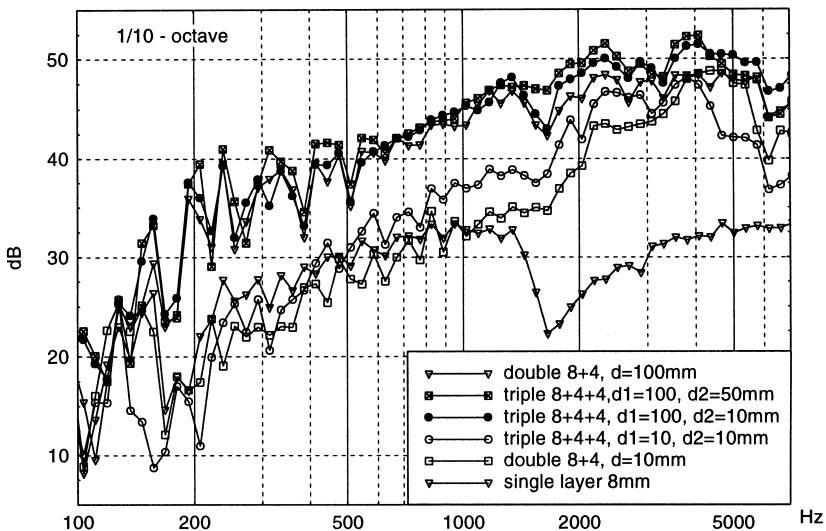


Fig. 9. Insulation curves. Single, double and triple glazed solutions.

The natural modes of the glass, arising from the transversal vibration of the panel under flexion [Eq. (7)], also influence the response. However, the dominance of the dynamic response of the excited natural vibrations modes of the testing rooms [Eq. (14)], does not allow easy detection of these modes in the acceleration spectra presented. It is only possible to identify some of these frequencies by resorting to the way in which the panel is displaced in the presence of a determined vibration mode (not shown).

Analysis of insulation curves reveals a disparity between the theoretical [Eq. (2)] and the experimental results. Bigger differences are found at frequencies above coincidence, while smaller differences only occur at frequencies appreciably below coincidence. It is common to use the mass law expression at frequencies below coincidence [17]. However, at low frequencies, where sound wave length is of the same order or exceeds the plate size, the sound transmission loss exceeds the mass law [Eq. (2)]. This phenomenon has its origin in the rigidity of the panel and has been addressed by several authors [18, 19].

The maximum dip due to coincidence effect does not occur at the critical frequency (f_c), it does so at a higher frequency. This was expected, because the critical frequency refers to the beginning of the coincidence phenomenon. Dips in insulation due to the coincidence effect, were more pronounced for the 4 mm panel, explained by its higher area to thickness ratio, which allows the easier propagation of flexion waves throughout its plane. Vibration of the glass panel shows that the dips in acoustic insulation are related to its movement. Vibration in the 4 mm panel is more marked at the higher frequencies, whereas in the 8 mm panel vibration spectrum, the lower frequencies are more pronounced. Above the critical frequency, the insulation curves exhibit slopes with an inclination close to 9dB/octave, as predicted by Eq. (6).

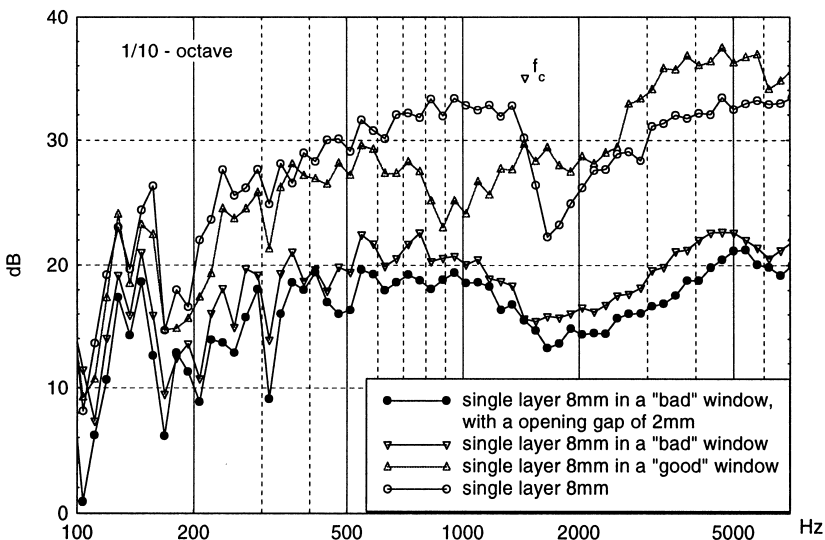


Fig. 10. Insulation curves. Single 8 mm glazed solution, with and without frame.

It can be further observed, comparing both experimental insulation curves with the theoretical mass law for frequencies below the critical, that the light panel glass (4 mm) performs as expected, while the panel 8 mm thick performs poorly. Quirt [17] registered a similar trend when measuring transmission loss data for three thicknesses of glass (3, 4 and 6 mm). Several authors [20, 21] have concluded that the so-called “baffle effect” and “niche effect” are presumably responsible for much of this deviation from Eq. (2).

The present experimental weighted sound reduction indexes obtained reflect a small variation for the panels 4 and 8 mm thick ($R_w=29$ dB and $R_w=30$ dB, respectively). In part, this may be explained by the decrease in the critical frequency with increasing mass, so that for heavier glass panels the coincidence dip has a greater effect within the frequency range, affecting the calculation of the weighted sound reduction index. Quirt [17] found a similar trend and his results indicate $R_w=30$ dB for a 4 mm glass.

For the various double-glazed solutions tested, only the results of the two different solutions with 8+4 mm glass are illustrated: one with a 10 mm air chamber thickness (Fig. 4) and the other with a 100 mm air chamber thickness (Fig. 5). In these cases, the equivalent sound pressure level L_{eq} measured in the emitting room reached 110 dB(A), as before. The experiments were also conducted with the 4 and 8 mm panes, facing the emitting and the receiving rooms, respectively.

Both the experimental and the theoretical insulation curves [Eq. (12)], are displayed. In addition, the theoretical curve branch valid for lower frequencies ($20 \log[(m_1 + m_2)f - 47]$, $f < 2f_{res}/3$) has been extended for higher frequencies as a dashed line.

As before, the experimental insulation curves display dips related to the natural resonance frequencies of the testing rooms [Eq. (14)], conditioning the sound insulation at low frequencies. Again, at very low frequencies, where the sound wave length exceeds the plate size, the sound transmission loss exceeds the theoretical prediction (see Figs. 2 and 3). As the frequency increases the experimental insulation curves register poorer results than predicted. Analysis of the results reveals that the double-glazed solution with the 100 mm air chamber thickness (Fig. 5) shows a better performance than the 10 mm air chamber thickness (Fig. 4). The latter case gives a performance even worse than that expected for a single panel made with a mass that equals the sum of the masses of the constituent single panels ($m=m_1+m_2$), (see dashed line).

For frequencies above $f_1=c/2d$, successive three-dimensional reflections occur inside the air chamber, giving rise to stationary waves. In this case the enclosed air space may be considered a reverberating space. Brekke [22] proposed a transmission loss model for the two-leaf partition given by

$$R = R_1 + R_2 + 10 \log(A/S) \quad (16)$$

where R_i ($i=1,2$) is the transmission loss for the leaf i , A is the equivalent absorption in the air cavity, and S is the area of the partition.

In his model, Brekke assumes that the partition panels do not contribute to cavity absorption. The application of this model to the double glazed solution with 100 mm air chamber thickness may better approach the experimental insulation curve. However, the precise value of the random incidence absorption coefficient for the perimeter surfaces of the air cavity is not known.

It can be further observed that the dips of insulation occurring at the critical frequencies of the two panels (f_{c1} and f_{c2}) are not as pronounced as before (see Figs. 2 and 3). Notice that a double-glazed solution tested [23] using 4 + 4 mm glass with a 10 mm air chamber thickness (not shown) displayed a bigger dip of insulation than a single glass solution 4 mm thick (Fig. 2) exhibited. This happens because the coincident effect occurs in both panels at the same frequency. The experimental weighted sound reduction index obtained ($R_w = 28$ dB) reflected this phenomenon, registering a value even smaller than that given by a single glass solution ($R_w = 29$ dB). The acceleration spectra curves collected at the central measurement point *C* again shows that bigger dips of insulation occur when larger accelerations are present (see Figs. 3 and 4). It can further be observed that the glass panel facing the receiving room (8 mm) registers a smaller vibration amplitude, as the result of the smaller energy incidence supplied by the insulation of the first panel.

Additional experimental tests were performed using double glazed panels of 4 and 8 mm thickness, where different air chamber thicknesses (air gaps) were used. As can be seen from Fig. 6, the weighted sound reduction indexes (R_w), calculated from the experimental insulation curves, give minimum values when the air chamber thickness ranges from 10 to 30 mm. Curiously, these are the dimensions currently used in air chambers of glazed solutions. The weighted sound reduction index improves as the air chamber thickness decreases significantly or increases to values close to or greater than 50 mm. A similar trend was observed by Quirt [17, 24]. However, the 3 dB increase of the weighted sound reduction index for doubling the separation, observed by Quirt, was only registered when we moved to larger air layer thicknesses.

Eq. (16) also predicts an improvement in insulation of 3 dB per doubling of interpane space. Our experimental results (not displayed) confirm an improvement of insulation close to 3 dB per doubling of air chamber thickness, for frequencies $f > c/2d$.

Regarding the triple glazed solutions tested, only the results for the triple panels made of 8 + 4 + 4 mm glass types with two $d_1 = d_2 = 10$ mm thick air chambers (Fig. 7), and the solution with the first air chamber $d_1 = 100$ mm thick and the second $d_2 = 10$ mm thick (Fig. 8) are presented. In these experiments, the panel 8 mm thick was placed facing the receiving room. Figs. 7 and 8 give the experimental insulation curves collected, the acceleration spectra of the 8 mm panel at its centre, and the theoretical insulation prediction, assuming the triple glazed apparatus as a single leaf with a mass equivalent to the sum of each individual panel mass. In the present case, the equivalent sound pressure level L_{eq} measured in the emitting room reached 114 dB(A). Again, dips of insulation are found at critical frequencies (f_{c1} , f_{c2} and f_{c3}), resonance frequencies of the dynamic system are built as three masses attached by springs [Eq. (13)], (f_{res1} and f_{res2}), and resonance frequencies are related to the

stationary waves inside the air chambers between the glass panels (f_1 , f_2 and f_3). The acoustic insulation results do not show significant improvement in comparison with the double glazed solutions, when the same thicknesses of air gap are used. The acceleration spectra show this behaviour, displaying a bigger amplitude when $d_1 = d_2 = 10$ mm.

Figs. 9 and 10 present the experimental insulation curves in bands of 1/10 octave obtained for different glazed solutions [24]. Comparing the curves in Fig. 9, one may find a similar behaviour for the solutions for double $[8 + (100) + 4]$ mm ($d_1 = 100$ mm) and triple $[8 + (100) + 4 + (d_2) + 4]$ mm ($d_1 = 100$ mm and $d_2 = 10$ mm, $d_2 = 50$ mm) glazed solutions, with weighted sound reduction indexes $R_w = 42$, 43 and 44 (dB), respectively. It is also possible to see similar behaviour in single glazed solutions (8 mm) and multiple glazed solutions with small air chambers ($[8 + (10) + 4]$ mm and $[8 + (10) + 4 + (10) + 4]$ mm) (especially for frequencies lower than 1000 Hz), registering weighted sound reduction indexes of $R_w = 30$, 32 and 33 (dB), respectively. Similar behaviour was found by Quirt [25], and this author concluded that sound transmission loss is very similar when the combined inter-pane spacing of the triple window matched the double glazing.

Fig. 10 shows the experimental insulation curves when a single layer glass panel, 8 mm thick, is fixed to the wall opening directly, and inside a window frame, as described earlier. Comparison between the experimental insulation curves obtained reveals that a much smaller coincidence dip occurred when the glass panel is inside a window frame. This behaviour may be explained by the smaller area of each panel used in the solution with a frame. Indeed, the coincidence dip is small when the ratio between the area and the thickness of the panel decreases, so the propagation of longitudinal plane waves decreases. Fig. 10, also displays the insulation curve obtained when the window is opened very slightly (2 mm). It is noticeable that this small gap produces a pronounced drop in insulation, leading to a weighted sound reduction index of $R_w = 18$ dB. A similar result is given when the glass panel is fixed to a poorly sealed frame ($R_w = 20$ dB). In contrast, the well-sealed window ($R_w = 29$ dB), reaches the performance of a single layer of glass without a frame ($R_w = 30$ dB).

5. Conclusions

The experimental results demonstrate that the predictive theoretical models described in this work are not close to the experimental results for many simple and double-glazed solutions. The smallest differences between the insulation predicted and achieved experimentally usually occur for single glazed panels.

Regarding the glazed solutions without frames, it can be concluded that the double glazing only exhibits better insulation behaviour than single panels if the air chambers are close to or greater than 50 mm thick, or if the air chambers are very small. With respect to double-glazing with two identical panels, the insulation dips for vibration eigenfrequencies are much greater than those found for solutions using glass of different thickness. Triple glazing offers no significant improvements over double-glazing; the improvements are not significant if we are looking at situations

where the larger air chamber in the triple glazed solution is the same as the air chamber in the double glazed solution.

In practice, the construction of double and triple glazing with thick air chambers, giving a high level of acoustic insulation, is possible by making double windows with separate frames. This type of solution may be useful where it is necessary to improve the acoustic insulation of an existing façade.

Analysis of the glazed solutions with frames enables us to see that acoustic insulation is generally poorer than that provided by glazed solutions without frames. The insulation values of the solutions with frames improve if the mass of the frame is relatively large and is well sealed. The application of high insulation glazed solutions thus implies the use of a high quality frame. A window with a very small opening may suffer a significant fall in acoustic insulation.

References

- [1] Cyril MH. Handbook of noise control. New York: McGraw-Hill Book Company, 1957.
- [2] Graff KF. Wave motion in elastic solids. New-York: Dover Publications, 1975.
- [3] Silva PM. *Acústica em Edifícios [Acoustics in Buildings]*. Lisbon, Portugal: Technical Information, Edifícios 8, LNEC, 1978.
- [4] Warnock ACC, Fasold W. Sound insulation: airborne and impact. *Encyclopedia of acoustics*, New York: Wiley-Interscience, 1997. Vol. 3: pp. 1129–61.
- [5] Beranek LL, Vér IL. *Noise and vibration control engineering*. New York: Wiley, 1992.
- [6] Rindel JH. Transmission of traffic noise through windows, influence of incident angle on sound insulation in theory and experiment. PhD thesis. Techn. Univ. Denmark, Report No. 9, 1975.
- [7] Sharp BH. Methods for the sound reduction of building elements. *Noise Control Engineering* 1978;11(2):53.
- [8] London A. Transmission of reverberant sound through double walls. *J Acoust Soc Am* 1950;44:270–8.
- [9] Goesele K. Prediction of the sound transmission loss of double partitions (without structureborne connections). *Acustica* 1980;45:218–27 (in German).
- [10] Bathe K-J. *Finite element procedures in engineering analysis*. Prentice-Hall, 1982.
- [11] Kuttruff H. Sound in enclosures. *Encyclopedia of acoustics*. New York: Wiley-Interscience, 1997. Vol. 3, pp. 1101–15.
- [12] Ouis D. Scattering by a barrier in a room. *Applied Acoustics* 1999;56:1–24.
- [13] Hammad RNS. Simulation of Noise Distribution in rectangular rooms by means of computer modelling techniques. *Applied Acoustics* 1988;24:211–28.
- [14] NP-2073:1986, *Acústica — Critérios de Quantificação do Isolamento Sonoro em Edifícios*. Correspondence:ISO717-1-2-3:1982 EQV.
- [15] Moser M. Vibration measurements and instrumentation. *Encyclopedia of acoustics*. New York: Wiley-Interscience, 1997. Vol. 2: pp. 857–69.
- [16] Tang WC, Zheng H, Ng CF. Low frequency sound transmission through close-fitting finite sandwich panel. *Applied Acoustics* 1998;55(1):13–30.
- [17] Quirt J. Sound transmission through windows I. Single and double glazing. *Journal of the Acoustical Society of America* 1982;72(3):834–44.
- [18] Gurovitch YuA. On low frequency sound insulation of rectangular plate. *Soviet Phys Acoust* 1978;26(3):508–15.
- [19] Novikov IL. Low-frequency sound insulation of thin plates. *Applied Acoustics* 1998;54(1):83–90.
- [20] Nilsson AC. Sound transmission through single leaf panels. Rep. 74-01, *Building Acoustics*, Chalmers University of Technology, Sweden, 1974.
- [21] Sewell EC. Transmission of reverberant sound through a single-leaf partition surrounded by an infinite rigid baffle. *J Sound Vibration* 1970;12:21–32.

- [22] Brekke A. Calculation methods for the transmission loss of single, double and triple partitions. *Applied Acoustics* 1981;14:225–40.
- [23] Mateus DMR, Tadeu, AJB. Acoustic behaviour of a single glazed opening. XXV IAHS World Housing Congress, Lisbon, Portugal, 1998. Vol 1, pp. 297–306.
- [24] Mateus DMR. Avaliação de Características Acústicas em Envidraçados Correntes. Dissertation submitted for Degree of Master in Civil Engineering (speciality: Construction Sciences), Civil Engineering Department, FCTUC, Coimbra, Portugal, 1998.
- [25] Quirt JD. Sound transmission through windows II. Double and triple glazing. *Journal of the Acoustical Society of America* 1983;74(2):534–42.